GEOLOGICA CARPATHICA, AUGUST 2005, 56, 4, 369–378

Reaction coronas around quartz xenocrysts in the basaltic andesite from Detunata (Apuseni Mountains, Romania)

NICOLAE HAR

Department of Mineralogy, "Babeş-Bolyai" University, Kogălniceanu Str. 1, 3400 Cluj Napoca, Romania; har@bioge.ubbcluj.ro

(Manuscript received May 20, 2004; accepted in revised form March 17, 2005)

Abstract: Olivine-bearing basaltic andesite from Detunata (Apuseni Mts, Romania) contains xenolithic material of sedimentary origin. Fragments of sandstone as well as isolated xenocrysts of quartz originated from sandstone, were identified. Reaction coronas consisting of pyroxene, tridymite, quartz fragments and glass are developed around some of the sandstone fragments and quartz xenocrysts, as a result of interaction between the xenolithic material and the host basaltic magma. Coronas can be divided into two distinctive parts. The outer one consists of a glassy matrix containing prismatic crystals of augite. The inner part of the coronas consists of isolated crystals of augite, fragments of quartz and tridymite in a glassy groundmass. Tridymite is also present along fractures in the quartz xenocrysts. Electron probe microanalysis and Raman spectroscopy were used to investigate the corona pyroxenes, glass, and silica polymorphs. The corona pyroxenes have chemical compositions typical for augite. The glass is highly siliceous (SiO_2 = 72.0–76.8 wt. %) as a result of quartz dissolution, high in alkalis (Na_2O = 1.38–3.22 wt. %; K_2O = 4.72–6.23 wt. %) and aluminum (Al_2O_3 = 9.31–12.18 wt. %). Tabular and twinned crystals of tridymite have a high content of alkalis ($Na_2O + K_2O$ = 0.30–0.39 wt. %) and alumina (Al_2O_3 = 0.54–0.86 wt. %) as compared to quartz xenocrysts. Raman spectra of tridymite show the most representative peaks at 403 and 422 cm^{-1}. The geochemistry of reaction corona, diffusion processes, and temperature were the controlling factors in the genesis of the newly-formed minerals in the reaction zones. The xenolithic material was partly assimilated, and represented an important source of Si^{4+}, Al^{3+}, Ca^{2+}, Mg^{2+}, Fe^{2+} and K^+. The spatial relationship between reaction pyroxenes and host basaltic andesite suggests that magma could also be the source for cations such as Ca^{2+}, Mg^{2+} and Fe^{2+}. The relatively higher content in alkalis of the volcanic glass from the basaltic andesite groundmass as compared to the glass of the corona suggests an enrichment in alkalis of the late differentiated magmatic melt which could represent the main source of alkaline cations (Na^+ and K^+). The genesis of the corona took place at low pressure, during the eruption of the basaltic magma. The presence of tridymite in the corona indicates temperatures higher than 870 °C while the presence of calcite in some xenoliths points to temperatures below 920 °C.

Key words: basaltic andesite, quartz xenocrysts, coronas of reaction, pyroxene, tridymite.

Introduction

The youngest Neogene–Quaternary calc-alkaline volcanic rocks cropping out in the Apuseni Mountains (Romania) (Fig. 1) are represented by the olivine-bearing basaltic andesites from Detunata (7.6 ± 0.4 Ma; Pécskay et al. 1995). They occur as two distinctive bodies: Detunata Goală (developed as polygonal columns) and Detunata Flocoasă. The bodies of olivine-bearing basaltic andesites were intruded into the flysch-type sedimentary deposits (Santonian–Maastrichtian) of the Bucium Unit. The magmatic rock contains xenoliths derived from the flysch. Different degrees of xenolith assimilation can be noticed. Some of them still preserve the textural and compositional features of the initial sedimentary rocks. Most of the xenoliths were fractured and partly assimilated by the basaltic magma. Thus, isolated xenocrysts of quartz occur in the resulted basaltic andesite rock. Millimeter-sized quartz xenocrysts (sometimes up to 10 mm) are randomly distributed in the rock. At the contact between quartz xenocrysts and basaltic magma, reaction coronas have developed. The coronas consist of pyroxene, glass, and SiO_2 polymorphs. Sato (1975), Grove et al. (1988), Backer et al. (1991), Luhr et al. (1995) and Har & Rusu (2000) described similar reaction products developed at the contact between quartz xenocrysts and basaltic melt.

Măldărescu (1978), based on microscopic data, reported the presence of pyroxene, glass and silica polymorphs (tridymite, metacristobalite and cristobalite) developed in connection with the assimilation of the "xenoliths of quartz", in basaltic andesite from Detunata.

The aim of the present study is to investigate, using modern techniques, the morphology of reaction coronas developed around quartz xenocrysts, as well as their chemistry and mineralogy, in order to assess the genetic conditions of the corona phases (minerals and glass) related to the reaction processes between basaltic magma and quartz xenocrysts.

Analytical techniques

Thin sections were investigated under a polarized microscope in order to study the reaction coronas developed around the quartz xenocrysts. Scanning electron microscope was used for imaging the corona pyroxenes and silica polymorphs, their mutual spatial relationships, and those with quartz xenocrysts and volcanic glass.

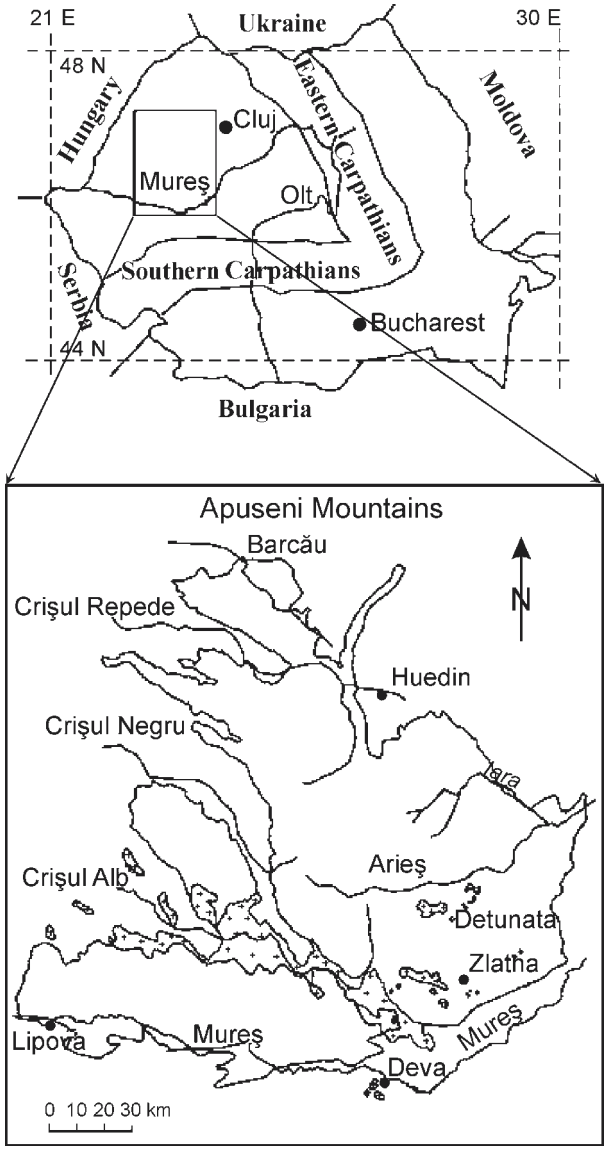

Fig. 1. Location of the Apuseni Mountains on the map of Romania (above) and position of the Neogene volcanism (+) and Detunata Massif in the Apuseni Mountains (below).

Pyroxenes, silica polymorphs, and the glass from the groundmass were analysed using a Cameca Camebax electron microprobe, with accelerating voltage of 15 kV, in the Department of Earth Sciences at Bristol University, UK. The take-off angle was 40° and the beam current was 15 nA for pyroxene, 25 nA for silica, and 10 nA for glass. The silica polymorphs were investigated also using a Raman spectrometer (He–Ne laser — 633 nm, laser spot < 2 μm) in the Physics Department of Bristol University.

Petrography and geochemistry of olivine-bearing basaltic andesite

The olivine-bearing basaltic andesites have porphyritic textures with intergranular–intersertal groundmasses. Due to the partial assimilation of the sedimentary material, specific compositional (hybrid) features of the volcanic rocks from Detunata can be observed. The following are present in the rock:

- minerals of igneous origin: plagioclase feldspars — 41 % (phenocrysts 83.6 % An–51.9 % An, microlites 70.2 % An–58.6%An), augite — 31 %, olivine (75 % Fo) — 3 %, oxidized amphibole — 6 %, titano-magnetite — 5 %, secondary minerals (chlorite, calcite) — 2 %, and volcanic glass — 7 % etc.
- phases related to the assimilation process of the xenoliths — 5 %: quartz xenocrysts (corroded by magma), minerals of reaction (pyroxene, silica polymorphs) and glass developed at the contact between basaltic rock and quartz xenocrysts.

The chemical composition of the volcanic rock from Detunata is typical for basaltic andesite (Table 1). However, its present composition, especially the SiO_2, Al_2O_3, K_2O and CaO contents, has been modified due to the assimilation of xenolithic material. Mineralogical features of the basaltic andesite corroborated with the observations on the xenoliths indicate that about 10 % of the present composition of the basaltic andesite is the result of the incorporation of xenolithic material into the magma; half of it was assimilated and the other half is still preserved as fragments of sandstone, quartz xenocrysts and new phases of the reaction corona. The total enrichment of the basaltic andesite in the main oxides, originated from the xenolithic material, is estimated as follows: SiO_2 — 5 %,

Table 1: Major element geochemistry of the basaltic andesite from Detunata (Har 2001) and its recalculated composition without xenolithic material.

	52	54	298	38	277	278	Average	Average recalculated
SiO_2	55.29	55.52	53.51	54.67	54.45	54.85	54.72	51.99
TiO_2	0.84	0.85	0.93	0.89	0.90	0.93	0.89	1.09
Al_2O_3	15.75	16.55	15.56	15.05	15.18	15.52	15.60	15.29
Fe_2O_3	6.80	7.05	7.31	6.90	6.79	6.90	6.96	8.56
MnO	0.13	0.10	0.13	0.14	0.11	0.14	0.13	0.16
MgO	6.09	5.96	6.33	6.81	6.46	6.45	6.35	7.81
CaO	9.49	9.58	9.52	9.84	9.38	9.74	9.59	8.54
Na_2O	2.71	1.96	2.53	2.77	2.70	3.01	2.61	3.21
K_2O	1.39	0.98	1.32	1.32	1.54	1.30	1.31	1.05
P_2O_5	0.21	–	0.22	0.24	0.24	0.25	0.23	0.28
H_2O	0.69	–	1.57	1.02	1.25	0.47	1.00	1.23
LOI	–	0.85	–	–	–	–	0.12	0.14
Total	99.39	99.40	98.93	99.65	99.00	99.56	99.51	99.35

Table 2: Chemical composition of the volcanic glass from the groundmass of the basaltic andesite (wt. %).

	1	2	3	4	5	6	7	8	9	10
SiO_2	67.86	66.24	63.64	67.95	67.55	67.00	65.62	67.78	67.97	67.68
TiO_2	1.73	1.38	1.19	1.79	1.72	1.56	1.51	1.81	1.69	1.36
Al_2O_3	13.03	13.89	16.47	11.43	12.52	12.77	13.66	11.23	11.85	13.27
Cr_2O_3	0.04	0.01	0.00	0.00	0.04	0.00	0.04	0.05	0.00	0.00
FeO	3.08	2.66	2.41	3.17	2.93	3.00	2.83	3.35	3.12	2.52
MnO	0.04	0.04	0.06	0.13	0.12	0.11	0.09	0.07	0.10	0.02
MgO	0.34	0.29	0.29	0.37	0.28	0.36	0.33	0.50	0.39	0.26
CaO	1.89	2.20	4.09	0.90	2.01	1.37	2.07	0.95	1.08	1.89
Na_2O	3.77	3.49	3.84	3.25	3.51	3.61	3.79	3.07	3.20	3.43
K_2O	4.80	5.83	4.32	6.19	4.85	6.21	5.39	6.34	6.04	5.72
Total	96.58	96.01	96.32	95.18	95.53	95.98	95.33	95.14	95.43	96.14

Al_2O_3 — 2 %, K_2O — 2 %, and CaO — 1 %. Thus, on the basis of these data, the chemical composition of the volcanic rock was recalculated without the participation of the xenolithic material and the result is presented in Table 1.

The volcanic glass (aprox. 7 wt. %) is present in the groundmass of the basaltic andesite. The chemical composition of the volcanic glass is presented in Table 2. It is acidic in composition (SiO_2 = 63.63–67.95 wt. %) with total alkalis (Na_2O + K_2O) between 8.17–9.81 wt. %.

Petrography of the sedimentary xenoliths

The basaltic andesite from Detunata pierced the flysch-type deposits of the Bucium Unit, which consists of conglomerates, polygeneous breccias, sandstone and marls. During its ascension, the basaltic magma incorporated fragments of sedimentary rocks as xenoliths. Depending on the depth of incorporation and the temperature of the magma, the xenoliths underwent different degrees of transformation. Minor transformations are typical for the xenoliths from the margins of the magmatic body. They still preserved some of the textural (e.g. stratification) and mineralogical features of the sedimentary rocks. The south eastern part of the Detunata Goală contains the only outcrop where fragments up to 5 cm length of sedimentary xenoliths can be found (Fig. 2a). Macroscopically they are light grey and yellowish in colour. Under the microscope they show a "porphyritic" texture. Fragments of sandstone, isolated angular quartz and quartzite originating from sandstone are surrounded by an isotropic groundmass, which sometimes represents up to 50 % of the rock (Fig. 2b,c and d). Fragments of sandstone are well preserved and consist of quartz, lithic fragments of quartzite, and micas (muscovite, biotite sometime opacitized or transformed into chlorite) as terrigenous components, having quartziferous and calcitic cement. The isotropic groundmass consists of glass and opaque material. The presence of glass in the groundmass is the result of partial melting of the xenoliths after their incorporation by the basaltic magma as well as of the rapid quench of the magma at the contact with the xenolithic material.

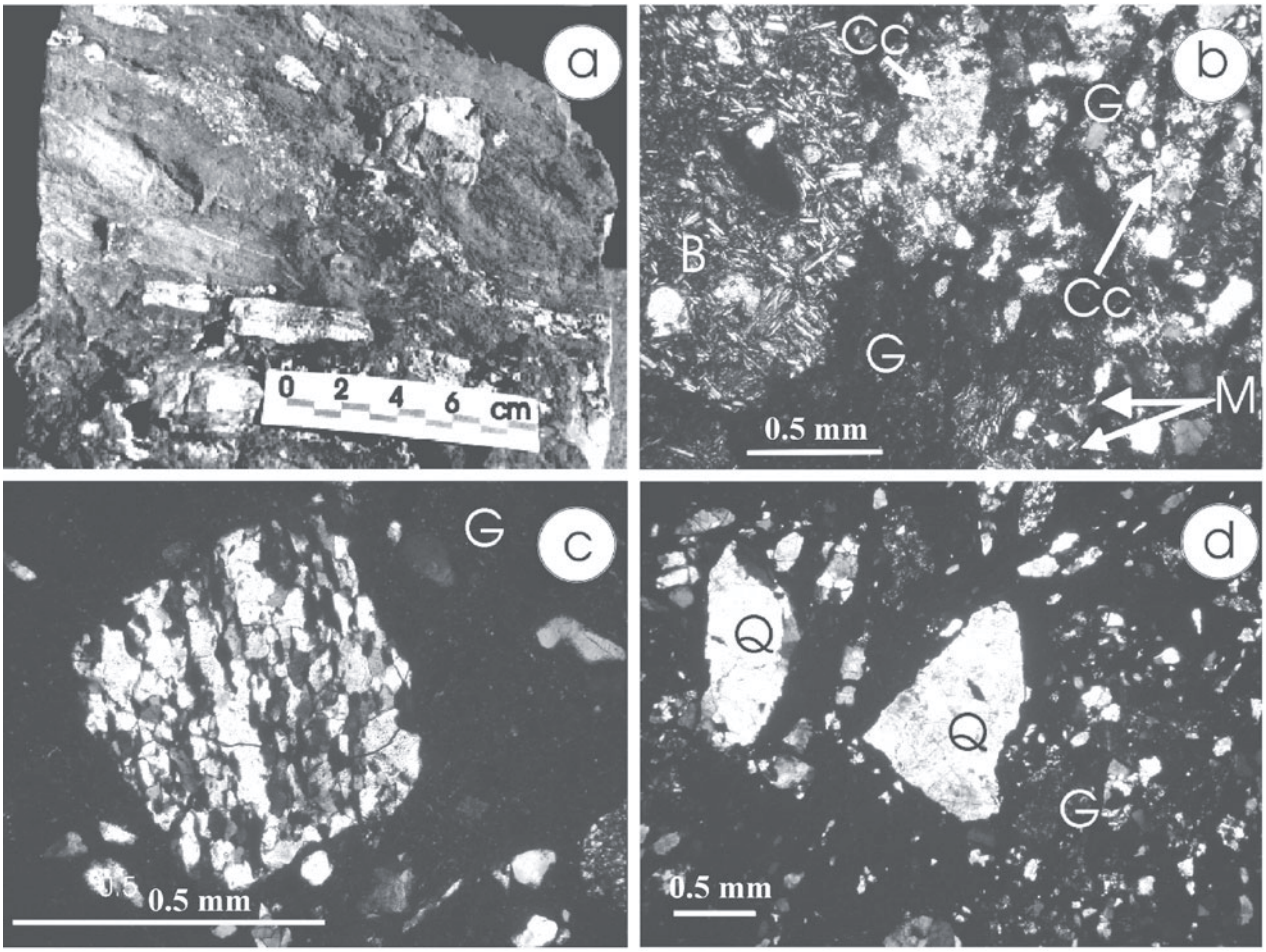

Fig. 2. Xenolithic material incorporated by the basaltic andesite from Detunata. **a** — Fragments of sandstone in volcanic material. **b** — Microphotograph showing a sandstone xenolith at the contact with the host basaltic andesite (B). The sandstone consists of quartz, micas (M), and calcite (Cc). The isotropic groundmass (G) is the result of partial melting of the xenolith. **c** — Fragment of quartzite originated from sandstone, into the isotropic groundmass (G). **d** — Isolated quartz (Q) into isotropic groundmass (G), as the result of partial melting of the sandstone.

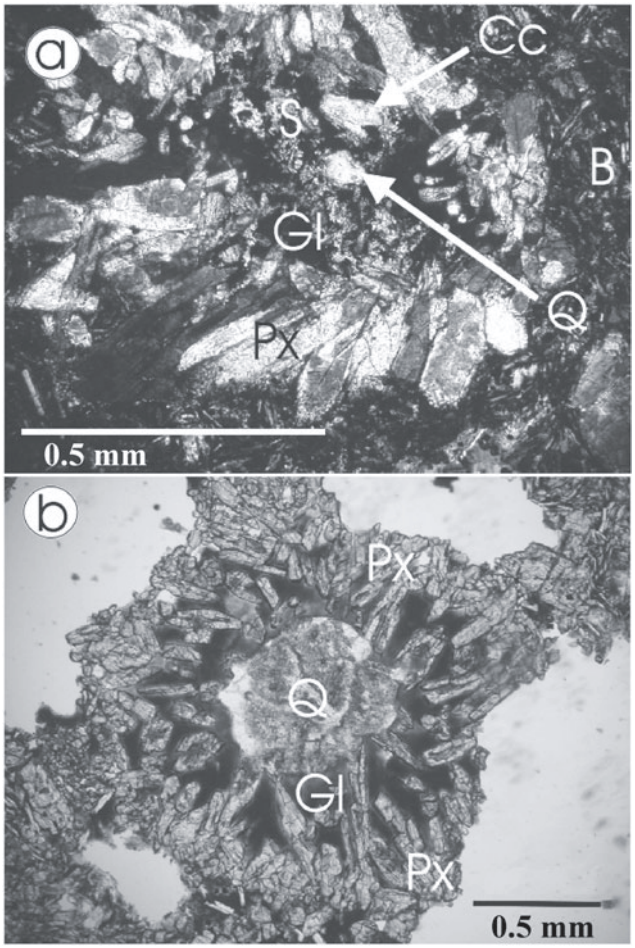

Fig. 3. a — Reaction corona consisting of pyroxene (Px) and glass (Gl) at the contact between basaltic andesite (B) and xenolithic sandstone (S). The sandstone consists of quartz (Q) and calcite (Cc). **b** — Isolated quartz xenocryst (Q) with reaction corona consisting of radial crystals of pyroxene (Px) and glass (Gl).

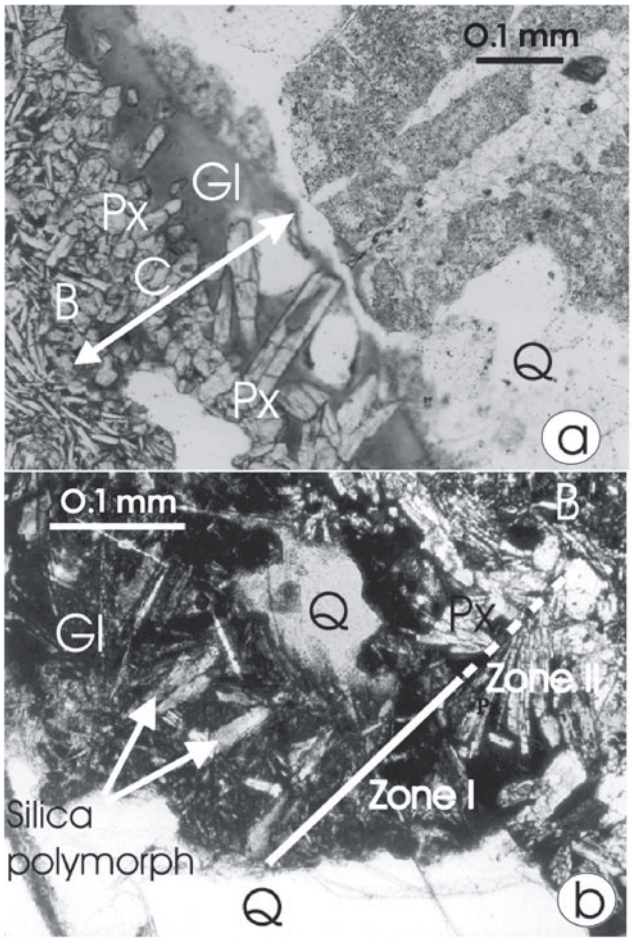

Fig. 4. a — Detailed microphotograph (ordinary light) of the reaction corona (C) with pyroxene (Px) and glass (Gl) developed between basaltic andesite (B) and quartz xenocrysts (Q). **b** — The zonality of the coronas: zone I consisting of tabular crystals of silica polymorph into a glassy groundmass (Gl) and zone II where pyroxenes are developed at the contact with the basaltic andesite (B), in the glass (Gl) of the corona. Due to the partial dissolution of the quartz xenocrysts (Q), isolated fragments of quartz are also present in the corona.

The xenoliths were partly assimilated and thus isolated fragments of sandstone and quartz are present in the host magmatic rock. Both fragments of sandstone (consisting of quartz, micas and calcite) and individual crystals of quartz, which appear as xenocrysts in the magmatic rock, reacted with the basaltic magma generating coronas of reaction (Fig. 3).

Description of the coronas

The best-developed are the coronas which surround the quartz xenocrysts. The anhedral form of quartz xenocryst (irregular in shape and corroded by the host magma) is the result of the dissolution processes, which took place at the contact with the basaltic melt. The coronas consist of different phases, most of them being the result of quartz dissolution and reaction with the basaltic magma (Fig. 4a,b). The coronas are variable in width. In some cases they are absent, but sometimes the width is up to 1 cm.

Coronas developed between quartz xenocrysts and the basaltic rock can be divided into two distinctive zones (Fig. 4b):

- Zone I (inner) — consists mainly of glass associated with crystals of silica polymorphs, isolated pyroxenes, and fragments of quartz. The aggregates of tabular crystals of silica polymorphs are concentrated at the edge of the quartz xenocrysts, in a glassy groundmass. Locally, at the edge of quartz some isotropic and colourless silica is also present. Some grains of pyroxene are developed as individual crystals in the glassy groundmass, but some of them grew up on the quartz xenocrysts.
- Zone II (outer) — is composed of well-developed pyroxenes in a glassy groundmass. The prismatic crystals of pyroxene are developed mainly perpendicular to the interface between the corona and the basaltic host-rock. In some cases there is only glass present in the outer part of the corona.

The quartz xenocrysts were partly broken and assimilated by the basaltic melt. This is evident from the presence of small fragments of quartz in the coronas (Fig. 5) as well as from the higher content of SiO_2 of glass of the corona as compared to the volcanic glass of the basaltic andesite. Due to the high

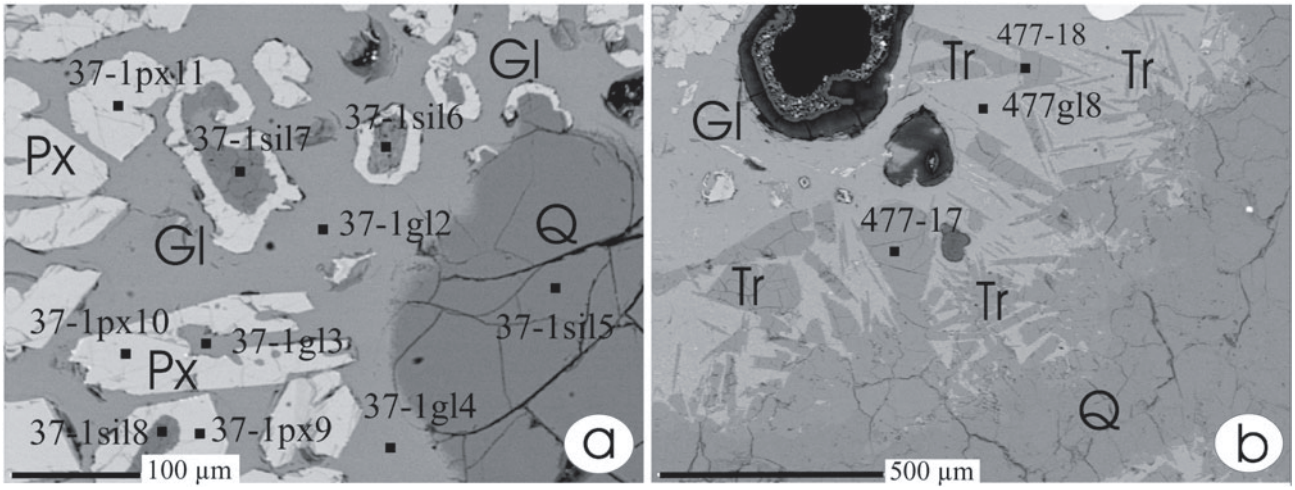

Fig. 5. SEM images of the inner part of the corona, close to the anhedral fragments of quartz xenocrysts (Q). **a** — Small fragments of quartz coated by the newly-formed skeletal pyroxene into the glassy groundmass (Gl) of the corona. **b** — Tabular and twinned crystals of tridymite (Tr) at the margin of the quartz grain (Q). The marked points represent the spots where the analyses were performed.

temperature of the basaltic magma, the dissolution processes took place along the quartz margins. Within the resulted silica-saturated melt, crystals of silica polymorphs were formed. Along internal fractures, where clusters of silica polymorphs crystals were also identified, quartz probably recrystallized.

Pyroxenes are developed mainly in the outer part of the coronas, at the contact with the basaltic rock (zone II), but they are present as isolated crystals in the inner part as well (zone I). The pyroxenes of zone II are prismatic in shape and form radial aggregates (Fig. 3b), usually perpendicular to the contact between the basaltic rock and the reaction rim.

In the inner part of the coronas the pyroxenes are prismatic or isometric in shape, isolated and unoriented, randomly distributed in the glassy groundmass. Nucleation of the pyroxene started homogeneously as individual crystals or on small preexisting fragments of quartz (Fig. 5a).

Composition of the coronas

Quartz xenocrysts and tabular crystals of silica polymorphs, glass, and pyroxenes from coronas were analysed by electron microprobe. The points selected for analyses are shown in Figs. 5 and 6.

Quartz and tabular silica polymorphs

The analyses of quartz were performed on the primary grains of the xenocrysts as well as on the small fragments from the inner parts of the coronas (zone I), especially on the isolated grains representing the substrate of the newly-formed pyroxene (e.g. Fig. 5a: 37-1sil 6, 37-1sil 7, 37-1sil 8 etc.). The results are reported in Table 3.

Significant differences in alkalis (Na_2O+K_2O) and Al_2O_3 contents can be noticed when comparing the analyses performed within the quartz grains (477-8, 37-1sil 2 and 37-1sil 5) with those from the margins, as well as from the isolated grains of the inner zone (I) of the coronas. Low alkali contents (Na_2O+K_2O = 0–0.03 wt. %) and Al_2O_3 (0.01–0.08 wt. %) are typical for the measured points inside the quartz grains. The external rims of the quartz xenocrysts, as well as the small quartz grains present in the inner area of the coronas are characterized by important increases of alkalis and Al_2O_3 contents (Fig. 7).

The analysed crystals of silica polymorphs are tabular in shape or twinned (triangular shape in section) and developed at the edge, or within fractures in quartz grains. Five tabular or twinned crystals of silica polymorphs were analysed: 477-9, 477-10, 477-11, 477-17 and 477-18 (Figs. 5b and 6a). The re-

Table 3: Chemical composition of the quartz xenocrysts (wt. %).

	477-8	477-12	477-13	37-1sil1	37-1sil2	37-1sil3	37-1sil4	37-1sil5	37-1sil6	37-1sil7	37-1sil8
SiO_2	97.70	97.28	98.15	97.99	97.99	96.67	98.55	99.23	94.31	98.97	98.34
TiO_2	0.03	0.11	0.15	0.16	0.00	0.11	0.21	0.02	0.37	0.02	0.00
Al_2O_3	0.08	0.56	0.47	0.50	0.01	0.72	0.47	0.02	0.81	0.06	0.03
Cr_2O_3	0.13	0.09	0.00	0.00	0.00	0.00	0.00	0.01	0.00	0.00	0.00
FeO	0.16	0.17	0.15	0.10	0.00	0.12	0.02	0.00	0.95	0.09	0.17
MnO	0.00	0.07	0.02	0.00	0.00	0.03	0.00	0.07	0.06	0.00	0.01
MgO	0.15	0.01	0.00	0.04	0.00	0.00	0.01	0.00	0.05	0.03	0.00
CaO	0.04	0.01	0.03	0.01	0.01	0.01	0.00	0.00	0.13	0.01	0.08
Na_2O	0.01	0.19	0.22	0.22	0.00	0.13	0.19	0.00	0.26	0.15	0.10
K_2O	0.02	0.15	0.11	0.12	0.00	0.17	0.10	0.00	0.32	0.02	0.00
Total	98.32	98.64	99.30	99.14	98.01	97.96	99.55	99.35	97.26	99.35	98.73

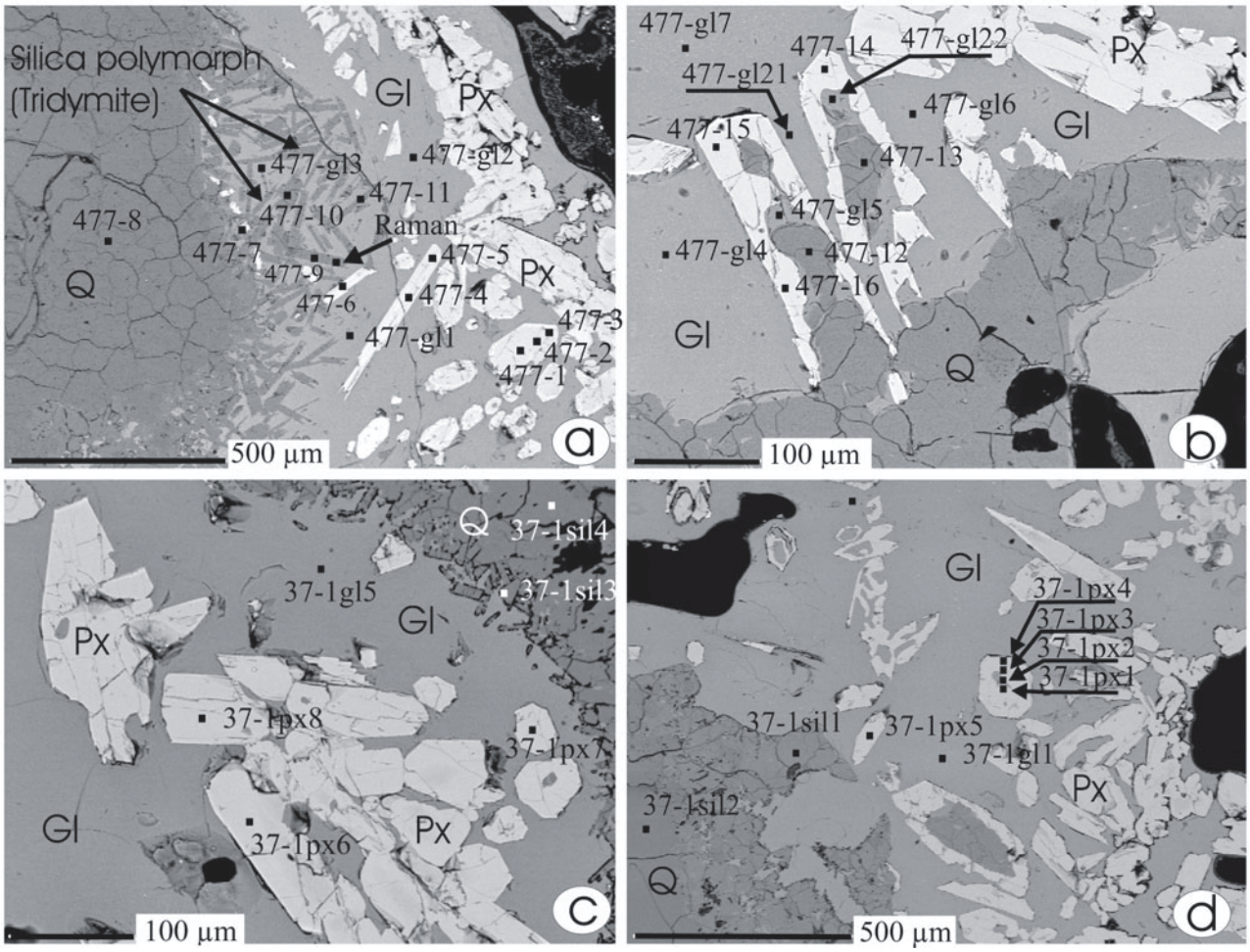

Fig. 6. Quartz xenocrysts (Q) and their reaction corona consisting of glass (Gl), silica polymorph (tridymite) and pyroxenes of reaction (Px), with the location of the investigated spots in the main phases of the corona.

sults are typical for tridymite (Table 4). The analysed crystals of tridymite show high contents of Na_2O, K_2O, and Al_2O_3 as compared to the quartz xenocrysts (Fig. 7). Moreover, the alkalis are more concentrated in the isolated quartz grains of zone I, in the outer rims of the quartz xenocrysts, as well as in the glass of the coronas.

Raman spectra of the silica polymorphs

In order to identify the silica polymorphs, Raman investigations in the range 0–1000 cm^{-1} were performed, although the range between 380 and 480 cm^{-1} is the most representative for the structures with six-membered rings, such as quartz and tridymite (Matson et al. 1986). Raman spectroscopy was performed on quartz xenocrysts as well as on tabular crystals of tridymite from the inner parts of the coronas. The Raman spectra of quartz show the most intense peaks at 128, 206, 265, 355, 464, 511, 696, 796, and 808 cm^{-1} (Fig. 8). The Raman patterns of tridymite contain peaks at 115, 403, 422, 537 and 593 cm^{-1} (Fig. 8), but all of them show smaller relative intensities compared with α-quartz. Raman measurements performed on silica polymorphs fit well with the data of Kingma & Hemley (1994) for α-quartz and only partly for tridymite (403 and 422 cm^{-1} peaks, which seem to be the most representative).

Table 4: Chemical composition of the tridymite (wt. %).

	477-9	477-10	477-11	477-17	477-18
SiO_2	97.50	97.26	96.93	97.36	97.49
TiO_2	0.07	0.11	0.12	0.03	0.07
Al_2O_3	0.55	0.77	0.86	0.54	0.68
Cr_2O_3	0.00	0.00	0.05	0.08	0.00
FeO	0.15	0.06	0.30	0.04	0.12
MnO	0.00	0.01	0.00	0.00	0.00
MgO	0.00	0.03	0.06	0.01	0.03
CaO	0.02	0.00	0.08	0.01	0.01
Na_2O	0.23	0.25	0.28	0.26	0.16
K_2O	0.14	0.19	0.19	0.13	0.14
Total	98.66	98.68	98.87	98.46	98.70

Glass

Glass is one of the main components and represents the groundmass of the coronas. Fifteen electron microprobe analyses of the glass were performed in different parts of the diffu-

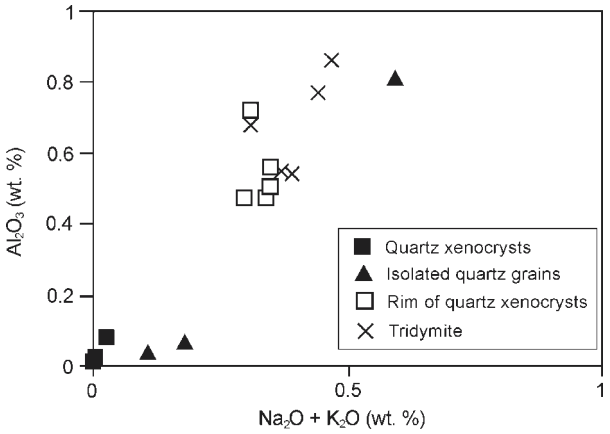

Fig. 7. Variation in alkalis and Al_2O_3 contents in the quartz xenocrysts, rim of the quartz xenocryst, the isolated quartz grains of the corona and tridymite.

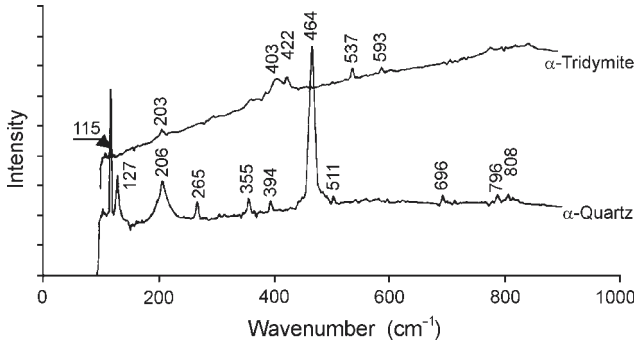

Fig. 8. Raman spectra of quartz xenocryst and tridymite from Detunata.

sion coronas (Figs. 5a and 6a,b,c and d). The results are presented in Table 5.

The glass of the coronas is highly siliceous in composition (SiO_2 = 70.35–76.87 wt. %) and also contains high levels of alkalis (Na_2O = 1.39–3.22 wt. %, K_2O = 4.73–6.23 wt. %) and Al_2O_3 (9.32–12.18 wt. %). A high content of alkalis is typical for Si-rich glass from such coronas (Sato 1975).

Pyroxenes

Clinopyroxene is also an abundant phase of the coronas. It is present in the inner reaction zones as isolated and randomly distributed crystals as well as in the outer zones at the contact with the basaltic host, where the crystals are usually prismatic in shape and form radial aggregates.

Electron microprobe analyses on the corona pyroxenes were performed in two different ways (Figs. 5a and 6a,b,c, and d):

- on profiles from the core to the rim of the crystal (in two differently oriented profiles on two different crystals). One profile was choosen longitudinally (along the c axis) of the crystal (Fig. 6a) and the second one transversally (from core to rim in a thin section perpendicular to the c axis; Fig. 6d) in order to illustrate the chemical changes during crystal growth (Table 6).
- as isolated measurements on different crystals of the coronas (Table 7).

The profiles for both crystals revealed very homogeneous compositions with no significant variations. Gentle variations in some elements (e.g. for SiO_2) could be the result of the local geochemistry and diffusion rates within the reaction zone, even if the increase in SiO_2 fits very well with the normal evolution of the crystallization process, as well as the dissolution processes of the quartz xenocrysts.

All the chemical analyses presented in Table 7 were performed in the cores of isolated crystals. The results show a very high homogeneity of the analysed crystals. Small differences in chemical composition may be the result of different rates of cation exchange in different parts of the diffusion coronas.

In order to identify the corona pyroxene species, their composition were recalculated in terms of Wo, En, and Fs contents (Table 8). According to the diagram of Morimoto et al. (1988), all the analysed crystals correspond to **augite**.

Discussion

Incorporation of the sedimentary xenoliths by the basaltic magma led to local geochemical changes. According to the depth of incorporation and the magma temperature, parts of the xenoliths were assimilated. The resulting quartz xenocrysts were also partly dissolved by the host magma and thus, the enrichment in SiO_2 of the surrounding melt took place. As compared to the volcanic glass of the basaltic andesite, the glass of the corona is more acidic and with smaller amounts of alkalis (Fig. 9).

The chemical composition of the glass from the coronas also shows an enrichment in alkalis and Al_2O_3 as compared to

Table 5: Chemical composition of the glass in the corona (wt. %).

	477gl1	477gl2	477gl3	477gl4	477gl5	477gl6	477gl7	477gl8	477-gl21	477-gl22	37–1gl1	37–1gl2	37-1gl3	37-1gl4	37-1gl5
SiO_2	73.89	74.90	73.29	72.28	75.31	74.29	72.03	72.99	72.37	76.87	70.35	72.99	72.00	73.59	74.62
TiO_2	0.36	0.45	0.51	0.82	0.64	0.76	0.78	0.33	0.70	0.52	0.89	0.81	0.81	0.83	0.61
Al_2O_3	10.09	9.32	9.68	11.68	9.73	10.60	12.18	10.61	12.00	9.83	12.17	10.13	11.85	10.52	9.57
Cr_2O_3	0.46	0.09	0.41	0.01	0.04	0.17	0.13	0.00	0.05	0.02	0.04	0.14	0.00	0.38	0.04
FeO	2.12	2.52	3.27	2.61	1.91	2.37	2.63	3.64	1.94	1.88	3.12	2.67	1.47	2.63	2.26
MnO	0.58	0.00	0.00	0.00	0.00	0.00	0.00	0.00	0.00	0.06	0.10	0.13	0.17	0.00	0.00
MgO	0.17	0.00	0.27	0.13	0.12	0.08	0.09	0.46	0.04	0.03	0.20	0.10	0.03	0.10	0.11
CaO	0.43	0.53	0.68	0.71	0.46	0.58	0.74	1.03	0.42	0.26	0.81	0.40	0.45	0.44	0.47
Na_2O	2.85	2.64	2.50	3.22	2.15	2.48	2.96	2.71	2.14	1.39	3.21	2.66	2.31	2.44	2.04
K_2O	4.73	4.83	4.93	5.67	5.15	4.91	5.35	4.64	5.30	4.96	5.80	5.11	6.23	5.37	5.33
Total	95.68	95.28	95.54	97.13	95.51	96.24	96.89	96.41	94.96	95.82	96.69	95.14	95.32	96.30	95.05

Table 6: Chemical composition of the coronas pyroxenes on longitudinal and transverse profile (wt. %).

	477-1	477-2	477-3	37-1px1	37-1px2	37-1px3	37-1px4
SiO_2	52.75	52.22	51.74	50.77	52.88	52.84	52.74
TiO_2	0.11	0.16	0.21	0.33	0.42	0.35	0.42
Al_2O_3	0.52	0.46	0.53	0.47	0.77	0.85	0.74
Cr_2O_3	0.00	0.00	0.00	0.06	0.00	0.04	0.00
FeO	9.24	9.06	9.50	9.70	9.57	9.72	9.44
MnO	0.43	0.25	0.36	0.45	0.38	0.31	0.28
MgO	14.83	14.52	14.40	15.01	15.39	15.72	15.58
CaO	21.12	21.39	20.87	20.56	20.41	20.41	20.71
Na_2O	0.34	0.34	0.30	0.30	0.27	0.30	0.30
K_2O	0.00	0.00	0.02	0.01	0.01	0.01	0.05
Total	99.34	98.40	97.93	97.66	100.10	100.55	100.26

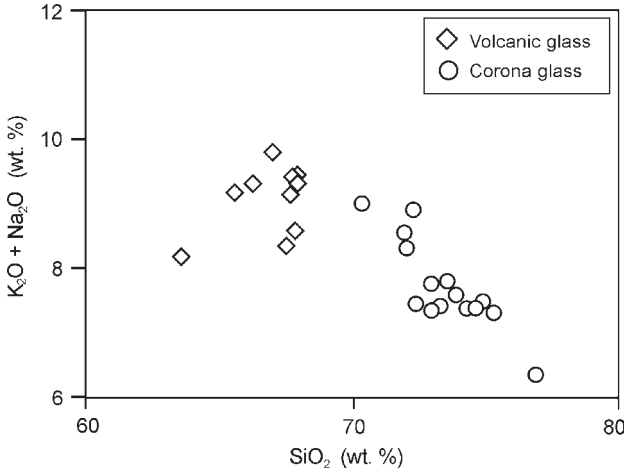

Fig. 9. SiO_2 vs. K_2O+Na_2O in the volcanic glass of the host basaltic andesite as compared to the glass of the corona.

the silica polymorphs of the corona. Analyses of the glass reveal average concentrations of alkalis (7.73 wt. %) and Al_2O_3 (10.66 wt. %) about 30 times the average level observed in quartz and tridymite (0.23 wt. % and 0.34 wt. % respectively) of the coronas. Both, the basaltic magma and the xenoliths, especially the phyllosilicate phases (muscovite, biotite), represent the source of alkalis and Al_2O_3. Alkali enrichment of tridymite is mainly dictated by the high partition coefficient for Na and K in silica-rich melt (derived from quartz dissolution) relative to the dominant basaltic melts of the host lava groundmass. Sato (1975) reported similar enrichments of alkali elements in the diffusion coronas developed around quartz xenocrysts from basaltic rocks of the Tertiary volcanic region in northeastern Shikoku in Japan.

Tridymite crystallized into the silica-saturated melt of the corona. The presence of Na and K in the corona melt favoured the crystallization of tridymite, which takes place more rapidly in the presence of such "mineralizing agents" (Heaney 1994). A positive correlation between Al_2O_3 and Na_2O+K_2O in the tridymite from coronas can be noticed. Such a correlation is typical for tridymite and it is likely to be due to the substitution of atomic Al to charge balance the substitution of Na, K, and Li in the silica polymorphs (Smith & Steele 1986). The relatively rapid quenching of the melt around the "cool" quartz xenocrysts, proved also by the presence of glass, inhibited the inversion of the tridymite to quartz.

Nucleation of the pyroxenes took place either homogeneously to form individual crystals, or on quartz grains, especially in the inner zone of the coronas. The crystals are invariably in contact with the glassy groundmass. The spatial association with the glass and the euhedral crystals of the corona pyroxenes, as well as their high compositional homogeneity suggest that the newly-formed crystals grew from melts that later quenched rapidly to glass. All clinopyroxenes from the corona are low in Al (Al_2O_3 = 0.21–0.85 wt. %) as compared with the pyroxene phenocrysts of the olivine-bearing basaltic andesite (Al_2O_3 = 2.39–2.54 wt. %; Har 2001). The low Al content reflects the high silica content of the local environment of the corona. The spatial position of the pyroxenes in the reaction zone developed between the host basaltic rock and the quartz xenocrysts suggests that both the basaltic melt and the glass of the corona represents the source of Ca, Mg, Al, and Fe, whereas the quartz xenocrysts represent the source of Si.

Table 8: The recalculated Wo, En and Fs end — members of corona pyroxenes (%).

Sample	Wo	En	Fs	Sample	Wo	En	Fs
37-1pr1	42.85	41.61	16.52	477-1	42.81	41.85	15.33
37-1pr2	41.14	43.17	15.67	477-2	43.76	41.33	14.89
37-1pr3	40.73	43.64	15.62	477-3	42.93	41.22	15.84
37-1pr4	41.43	43.36	15.20	477-4	42.46	41.15	16.37
37-1px5	41.87	42.64	15.48	477-5	41.91	41.11	16.97
37-1px6	39.39	44.49	16.10	477-6	42.11	39.89	17.99
37-1px7	40.76	44.27	14.96	477-7	43.02	38.40	18.56
37-1px8	41.46	42.88	15.65	477-14	43.88	39.95	16.15
37-1px9	40.71	43.45	15.82	477-15	41.40	41.77	16.82
37-1px10	40.12	44.11	15.68	477-16	42.50	41.09	16.40
37-1px11	41.14	43.176	15.67				

Table 7: Chemical composition of isolated crystals of pyroxenes in corona (wt. %).

	477-4	477-5	477-6	477-7	477-14	477-15	477-16	37-1px5	37-1px6	37-1px7	37-1px8	37-1px9	37-1px10	37-1px11
SiO_2	51.51	52.40	52.06	51.65	51.96	52.09	52.60	52.74	52.61	52.38	52.48	52.58	52.47	52.44
TiO_2	0.13	0.17	0.11	0.06	0.23	0.39	0.37	0.34	0.34	0.27	0.35	0.37	0.36	0.45
Al_2O_3	0.21	0.38	0.23	0.41	0.35	0.58	0.41	0.44	0.46	0.52	0.54	0.49	0.47	0.62
Cr_2O_3	0.00	0.15	0.03	0.00	0.05	0.00	0.03	0.00	0.12	0.01	0.00	0.04	0.03	0.00
FeO	9.90	11.18	11.57	12.75	9.75	10.27	10.11	9.55	9.71	9.05	9.71	9.76	9.72	9.27
MnO	0.32	0.45	0.61	0.63	0.41	0.34	0.33	0.36	0.25	0.38	0.33	0.28	0.33	0.40
MgO	14.41	14.47	13.91	13.22	15.12	15.80	15.69	15.32	15.46	15.67	15.44	15.49	15.90	15.64
CaO	20.70	20.52	21.44	20.62	21.28	20.41	21.14	20.94	21.05	21.08	20.77	21.19	21.08	21.02
Na_2O	0.32	0.33	0.30	0.33	0.32	0.34	0.31	0.31	0.24	0.30	0.29	0.30	0.30	0.29
K_2O	0.00	0.06	0.03	0.02	0.04	0.01	0.02	0.00	0.01	0.02	0.00	0.00	0.01	0.03
Total	97.50	100.11	100.29	99.69	99.51	100.23	101.01	100.00	100.25	99.68	99.91	100.50	100.67	100.16

It is very difficult to appreciate the intensity of diffusion of some cations from the magma as long as it must have been partly crystallized when the xenoliths were incorporated. Several evaluations regarding the participations of phases in reaction corona indicate the following aproximative amounts: glass — 55 %, pyroxene — 40 % and tridymite — 5 %. Taking their participation into account the weighted average chemical composition of the corona was calculated: SiO_2 = 66.17 wt. %, TiO_2 = 0.47 wt. %, Al_2O_3 = 6.09 wt. %, Cr_2O_3 = 0.08 wt. %, FeO = 5.33 wt. %, MnO = 0.18 wt. %, MgO = 6.10 wt. %, CaO = 8.66 wt. %, Na_2O = 3.91 wt. %, and K_2O = 2.79 wt. %. The results point out an enrichment of the corona in SiO_2, K_2O and Na_2O as compared with the host basaltic andesite, similar values of MgO, and depletion in Al_2O_3.

Conclusions

Olivine-bearing basaltic andesites from Detunata (Apuseni Mountains, Romania) contain xenoliths of sedimentary rocks (sandstone) and xenocrysts of quartz as the result of partial assimilation of the xenoliths. Both xenoliths and xenocrysts of quartz, randomly distributed in the basaltic andesite rock, underwent various processes:

- partial melting of the xenoliths and dissolution of quartz led to the enrichment in SiO_2 and alkalis of corona melt;
- tridymite crystallized into high silica environment of the corona;
- reactions with the basaltic melt led to the formation of corona pyroxenes (augite);
- assimilation, resulting in compositional changes of the magma.

The glass, which represents the groundmass of the reaction zone, was formed at the contact between the basaltic melt and "cold" quartz xenocrysts. Thus, surrounding the quartz xenocrysts, coronas consisting of glass, fragments of quartz, tridymite, and augite are present.

During the formation of the coronas, a cations exchange between the basaltic magma and the melt of the corona took place. The cation exchange was controlled by the specific physical (especially temperature, pressure, time from incorporation of xenoliths and the growth of the corona pyroxenes) and geochemical conditions existing in the reaction zone.

Luhr et al. (1995) concluded that for a longer reaction time, Al-poor pyroxene crystallizes from centres on the outer corona margins. Such spatial distribution of corona pyroxenes of reaction is very common at Detunata (Fig. 3b). The dissolution rate of quartz in a basaltic melt is strongly controlled by the crystallization state of the melt (Donaldson 1985). A higher dissolution rate is present if the basaltic melt is superheated (above the liquidus temperature) than in the case of a partly crystallized melt. The presence of olivine and pyroxene as phenocrysts in the basaltic andesite from Detunata suggests that the melt was partly crystallized when quartz was incorporated. On the other hand, the presence of glass in the groundmass of the host-rock indicates a high rate of post-eruptive cooling. Thus, the reaction process seems to be mainly controlled, beside geochemical conditions, by the time interval between the incorporation of the quartz xenocrysts and the eruption of the magma. The presence of xenolithic sandstone, quartz xenocrysts, with and without reaction coronas at Detunata indicates variable depth of quartz incorporation by the melt.

The diffusion of Si^{4+} from the lattice of quartz into the corona generates the acidic composition of the melt in the reaction zone. During dissolution, Si^{4+} diffused from the quartz xenocrysts towards the neighbouring melt. K^+ and Al^{3+} diffused in the opposite direction (from the melt towards the quartz xenocrysts) as shown by the high amounts of K_2O and Al_2O_3 at the external zone of quartz, as compared to those in the centre (see Fig. 7).

Different processes have controlled the geochemistry of the reaction corona:

1. Partial melting of the sandstone xenoliths followed by the quartz dissolution. The fusion of the hydrous phyllosilicate phase (muscovite, biotite) could be an important source of K^+.

2. Metasomatic processes which took place at the contact between the quartz xenocrysts and the basaltic melt:

— Si^{4+} was released from the quartz into the reaction zone;

— The cation exchanges between the magma and the melt of the corona. The diffusion between the two liquids (the basaltic vs. the corona melt) induced a permanent change in the chemical composition of the melt in the neighbourhood of the quartz xenocrysts. The process decreased in intensity progressively as the pyroxene crystals, constituting a diffusion barrier, started to form; in parallel, the chemical heterogeneity of the two liquids decreased too.

— The highest values of K_2O and Na_2O in the corona also suggest the existence of an alkaline front diffused from the basaltic melt into the corona zone.

3. The crystallization of tridymite and pyroxenes of reaction from the melt. The presence of alkalis in the corona favoured the crystallization of tridymite from the silica-saturated melt next to the quartz xenocrysts and thus, a high content of alkalis ($Na_2O + K_2O$ = 0.30–0.47 wt. %) and aluminum oxide (Al_2O_3 = 0.54–0.86 wt. %) in the tridymite can be noticed. Schneider (1986) explained the relationship of the alkalis and aluminum oxide in the tridymite as the result of the entry of sodium and potassium into the structural channels and voids of the tridymite. Aluminum substitution for silicon in the oxygen tetrahedra, in the neighbourhood of alkali ions centers was required to maintain charge balance due to alkali ion entry into the structure of the tridymite. The glassy groundmass of the corona is also enriched in alkalis (Na_2O = 1.39–3.21 wt. %; K_2O = 4.64–6.23 wt. %), aluminum oxide (Al_2O_3 = 9.32–12.18 wt. %), and SiO_2 (70.35–76.87 wt. %). Dissolution of quartz is responsible for the acidic nature of the glass, while the fusion of hydrous phyllosilicate phases (e.g. muscovite, biotite) as well as the diffusion of K_2O, and Na_2O from the basaltic melt led to the enrichment of glass in these components. The calcite from xenoliths represents the source of Ca^{2+}. The diffusion of Si^{4+}, Al^{3+}, Ca^{2+} and Mg^{2+} towards the pyroxene nucleation centres leads to the growth of pyroxene crystals (augite) in the acidic melt. The pyroxenes were formed mainly at the contact with the basaltic magma. Isolated crystals of augite were also formed inside the melt of the diffusion corona, *via* nucleation as individual pyroxene crystals, or as overgrowth on quartz fragments (Figs. 5a and 6b).

The genesis of the reaction corona took place at low pressures and at temperatures around 900 °C. The reaction processes took place while the basaltic magma erupted. Such conditions indicate a low pressure of the magma — xenolithic material system. The presence of tridymite in the reaction corona indicates temperatures higher than 870 °C, while the presence of calcite in some xenoliths with typical reaction coronas point out temperatures below 920–940 °C. Higher temperatures could be reached by the earlier incorporated xenoliths which underwent partial melting, the quartz xenocrysts representing practically the unmelted part of the xenolith (e.g. restite).

Acknowledgments: I acknowledge the support of the European Community Access to Research Infrastructure action of the Improving Human Potential Program, contract HPRI-CT-1999-00008 awarded to Prof. B.J. Wood (EU Geochemical Facility, University of Bristol). All my thanks are due to Dr. Stuart Kearns and Dr. John Dalton for their assistance during electron microprobe analyses and Raman spectroscopy at the University of Bristol (UK).

I gratefully acknowledge Dr. Patrik Konečný and Dr. Peter Luffi for the careful review of the manuscript and their pertinent observations. Special thanks to Dr. Ben Williamson (NHM London — UK, Department of Mineralogy) and Dr. Dana Pop ("Babeş-Bolyai" University, Department of Mineralogy) for their careful review of the English version of the manuscript.

References

Backer M.B., Grove T.L., Kinzler R.J., Donnelly-Nolan J.M. & Wandless G.A. 1991: Origin and compositional zonation (high-alumina basalt to basaltic andesite) in the Giant Crater lava field, Medicine Lake volcano, northern California. *J. Geophys. Res.* 96, 21819–21842.

Donaldson C.H. 1985: The rate of dissolution of olivine, plagioclase and quartz in a basalt melt. *Mineral. Mag.* 69, 683–693.

Grove T.L., Kinzler R.J., Backer M.B., Donnelly-Nolan J.M. & Lesher C.E. 1988: Assimilation of granite by basaltic magma at Burnt Lava flow, Medicine Lake volcano, northern California: decoupling of heat and mass transfer. *Contr. Mineral. Petrology* 99, 320–343.

Har N. 2001: The alpine basaltic andesites from Apuseni Mountains. *Casa Cărţii de Ştiinţă*, 1–214 (in Romanian).

Har N. & Rusu A.M. 2000: Diffusion coronas around quartz xenocrysts in the basaltic andesite from Căpuş (Cionca Hill, Gilău Mountains — Romania). *Studia Universitatis "Babeş-Bolyai"*, *Geologia* XLV/1, 35–45.

Heaney P.J. 1994: Structure and chemistry of the low-pressure silica polymorphs. In: Heaney P.J., Prewitt C.T. & Gibbs G.V. (Eds.): Silica-physical behavior, geochemistry and materials applications. *Rev. in Mineralogy* 29, 1–32.

Kingma K.J. & Hemley R.J. 1994: Raman spectroscopic study of microcrystalline silica. *Amer. Mineralogist* 79, 269–273.

Luhr F.J., Pier G.J. & Aranda-Gomez J.J. 1995: Crustal contamination in early Basin and Range hawaiites of the Los Encinos Volcanic Field, central Mexico. *Contr. Mineral. Petrology* 118, 321–339.

Matson D.W., Sharma K.S. & Philpotts J.A. 1986: Raman spectra of some tectosilicates and of glasses along the orthoclase–anorthite and nepheline–anorthite joins. *Amer. Mineralogist* 71, 649–704.

Măldărescu I.1978: Contributions to the knowledge of the basalt with xenoliths of quartz from Detunata. *St. şi Cerc. de Geol., Geofiz. şi Geogr.* 23, 2, 167–334 (in Romanian).

Morimoto N., Fabries J., Ferguson A.K., Ginzburg I.V., Ross M., Seifert F.A., Zussman J., Aoki K. & Gottardi G. 1988: Nomenclature of pyroxenes. *Amer. Mineralogist* 73, 1123–1133.

Pésckay Z., Edelstein O., Seghedi I., Szakács A., Kovacs M., Crihan M. & Bernad A. 1995: K-Ar datings of Neogene–Quaternary calc-alkaline volcanic rocks in Romania. In: Downes H. & Vaselli O. (Eds.): Neogene and related magmatism in the Carpatho-Pannonian Region. *Acta Vulcanol.* 7, 2, 53–61.

Sato H. 1975: Diffusion coronas around quartz xenocrysts in andesite and basalt from Tertiary Volcanic Region in Northeastern Shikoku, Japan. *Contr. Mineral. Petrology* 50, 49–64.

Smith J.V. & Steele I.M. 1986: Chemical substitution in silica polymorphs. *Neu. Jb. Mineral. Mh.* H.3, 137–144.